Journal of the European Ceramic Society 37 (2017) 2227–2234

Contents lists available at www.sciencedirect.com

Journal of the European Ceramic Society

journal homepage: www.elsevier.com/locate/jeurceramsoc

Feature article

Novel 'inorganic gel casting' process for the manufacturing of glass foams

Acacio Rincón[a], Giovanni Giacomello[b], Marco Pasetto[b], Enrico Bernardo[a,*]

[a] Department of Industrial Engineering, University of Padova, Italy
[b] Department of Civil, Environmental and Architectural Engineering (ICEA), University of Padova, Italy

ARTICLE INFO

Article history:
Received 5 October 2016
Received in revised form 4 January 2017
Accepted 8 January 2017
Available online 12 January 2017

Keywords:
Gel casting
Alkali activation
Glass foams

ABSTRACT

A new technique for the production of glass foams was developed, based on alkali activation and gel casting. The alkali activation of soda-lime waste glass powders allowed for the obtainment of well-dispersed concentrated suspensions, undergoing gelification by treatment at low temperature (75 °C). An extensive direct foaming was achieved by mechanical stirring of partially gelified suspensions, comprising also a surfactant. The suspensions were carefully studied in terms of rheological behavior, so that the final microstructure (total amount of porosity, cell size) can be directly correlated with the degree of gelification.

A sintering treatment, at 700–800 °C, was finally applied to stabilize the foams, in terms of leaching of alkaline ions. Considering the high overall porosity (88–93%), the newly obtained foams exhibited a remarkable compressive strength, in the range of 1.7–4.8 MPa.

1. Introduction

The recovery of glass in differentiated urban waste collection, in order to manufacture new glass containers ("closed loop recycling"), has been implemented with success in the last years, reaching a rate of 73% of the overall amount glass packaging of the European Union in 2015 [1]. The approach is undoubtedly favourable, in saving both energy and raw materials [2] but it cannot be extended further, due to the need for an expensive and difficult sorting step, to be applied to the collected cullet, aimed at separate glass pieces with different colours and remove metal, plastic or ceramic impurities. A glass fraction, in which these impurities are concentrated, remains practically useless and it is known to be mostly landfilled [3,4]. It is not surprising, as a consequence, that glass cullet should be considered also is in a condition of "open loop recycling", i.e. re-use in articles different from the original ones, also termed "down-cycling", starting from value-added products, like glass foams [5].

Glass foams (or cellular glasses) represent a fundamental class of glass-based building materials. They are known to offer high surface area, high permeability, low density, low specific heat, high thermal and acoustic insulation and high chemical resistance; contrary to polymeric cellular materials, glass foams are non-flammable and flame resistant, chemically inert and not toxic, rodent and insect resistant, bacteria resistant, water and vapour resistant [6]. Unlike most glass-based objects, glass foams are not manufactured by means of a melting process, but generally depend on the sintering of recycled glass powders. The foaming depends on a delicate balance between viscous flow sintering and gas evolution, in turn determined by oxidation or decomposition reactions of additives mixed with glass powders [6].

As thermally insulating materials, glass foams contribute positively to energy saving and reduction of CO_2 emissions, but the same foaming reactions have a disputable environmental effect, since they occur at temperatures generally exceeding 850 °C (for common soda-lime glass), and imply energy dissipations in order to be effective. In the case of oxidation reactions, as an example, the homogeneity of foaming depends on the availability of oxygen not only from the atmosphere, but also "in situ" (as done by Pittsburgh Corning for the production of the well-known Foamglas ®, from glass powders added with carbon black [6,7]). This can be achieved by mixing recycled glass with an "oxidized glass", rich in ferric and manganic oxides (releasing oxygen upon firing, by conversion into ferrous and manganous oxides), that must be specifically prepared (with significant energy consumption associated with glass melting). An alternative is represented by oxidizing compounds as additive in mixtures of glass and foaming agent [8].

The present paper is essentially aimed at presenting a new approach to glass foams implying a dramatic revision of the foaming process, starting from alkali activation of soda-lime glass powders. The alkali-activation is actually receiving a growing

* Corresponding author at: Department of Industrial Engineering, University of Padova, Via Marzolo 9, 35131 Padova, Italy.
E-mail address: enrico.bernardo@unipd.it (E. Bernardo).

http://dx.doi.org/10.1016/j.jeurceramsoc.2017.01.012

interest in the fields of ceramics. Usual alkali-activated materials, generally known as "geopolymers", are produced through the reaction of an alumino-silicate raw material with an alkaline compound, which is typically a concentrated aqueous solution of alkali hydroxide or silicate [9]. The dissolution of the alumino-silicate component determines the release of 'inorganic oligomers' (molecules with few Si^{4+} and Al^{3+} ions mutually bonded by bridging oxygens, with OH terminations) in the aqueous solution, later subjected to condensation reactions, with water release and formation of a gel, at low temperature (room temperature or typically a temperature below 100 °C). Alumino-silicate raw materials, such as metakaolin, are known to yield a 'zeolite-like' gel, consisting of a continuous, three-dimensional alumino-silicate network, amorphous or crystalline [9]. The network features the bridging of $[SiO_4]$ and $[AlO_4]$ tetrahedra, the latter being formed by the presence of alkali ions in the surrounding spaces, for the charge compensation. The alkali ions remain substantially 'trapped' in the alumino-silicate network, for an optimum Al_2O_3/SiO_2 balance in the raw materials, with the achievement of chemically stable products. The stability is further confirmed by the possible entrapment of pollutants, starting from industrial by-products as part of the raw materials [10]. It should be noted that a gel is formed even from formulations with different Al_2O_3/SiO_2 balances; as an example, CaO-rich formulations do not yield a 'zeolite-like' gel, but provide a condensation product that could be termed 'tobermorite-like' gel, given the analogy with the products of cement hydration [9]. The term 'inorganic polymer' may be used to identify the products, independently from the structure [9,11].

The concept of alkali activation and 'inorganic polymerization' is open also to glasses, as raw materials. Glasses with engineered chemical composition (alumino-silicate glasses) can be used as precursors for geopolymer-like materials [12–14], to be used as new binders for the building industry, according to the formation of sodium alumino-silicate hydrate (N–A–S–H) and calcium alumino-silicate hydrate (C–A–S–H) gels. With proper molecular balances between different oxides, both strength and chemical stability are maximized. Recycled glass can be used as a component of mixtures yielding geopolymers [15–17]; if a zeolite-like gel is not the target, soda lime-glass cullet, activated with sodium or potassium hydroxide solutions, can be used as the only component. The so-obtained 'glass-based mortars', cured at 40–60 °C, achieve good mechanical strength (e.g. compressive strength of 50 MPa), but limited durability [18].

The present investigation recovers the idea of glass-based mortar, but not as a final product. On the contrary, the gel provided by activated soda-lime glass powders is used as an intermediate product for the foaming. As previously shown for highly porous geopolymers, air may be trapped by mechanical stirring of mixtures at the first stages of gelification, with the support of a surfactant [19]; the setting of the mixtures determines the 'freezing' of the cellular structure. In other words inorganic polymers may replace the complex mixture of organic compounds typically applied for the setting of aqueous slurries, in 'conventional' gel casting (also applied to glass powders, for the manufacturing of bioactive glass-ceramic foams [20]). A sintering treatment, at 700–800 °C, was finally applied to convert highly porous 'glass-based mortars' into glass foams, limiting the leaching of alkaline ions.

2. Experimental procedure

Soda-lime glass (later referred to 'SL'; chemical composition [21]: SiO_2 = 71.9 wt%, Na_2O = 14.4%, K_2O = 0.4%, CaO = 7.5%, MgO = 4.0%, Fe_2O_3 = 0.4%, Al_2O_3 = 1.2%) from crushed glass containers was used as starting material. It was provided by the company SASIL SpA (Biella, Italy) in the form of fine powders (mean particle size of 75 μm), corresponding to the glass fraction that remains practically unusable, after colour selection and removal of metallic and polymeric residues, due to the presence of ceramic contaminations.

As received fine powders were inserted in an aqueous solution containing 2.5 M KOH (reagent grade, Sigma– Aldrich, Gillingham, UK), for a solid loading of 65 wt%. The glass powders were subjected to alkaline attack for 3 h, under low speed mechanical stirring (500 rpm). After alkaline activation, the obtained suspension of partially dissolved glass powders was cast in closed polystyrene cylindrical moulds (60 mm diameter), and cured at 75 °C.

The gelation process was evaluated at different times by controlling the rheological behaviour. Suspensions were extracted from the moulds and analysed by means of a plate–plate rheometer (Anton Paar MCR 302, Paar Physica, Austria), operating with controlled shear rate (increase from 0 to 500 s^{-1} in 3 min, stabilization at 500 s^{-1} for 1 min and decrease from 500 to 0 s^{-1} in 3 min), at room temperature. Regression analyses were performed considering only the up-curves of the corresponding rheograms.

Gels obtained at different curing times were first added with 4 wt% Triton X-100 (polyoxyethylene octyl phenyl ether – $C_{14}H_{22}O(C_2H_4O)_n$, n = 9–10, Sigma-Aldrich, Gillingham, UK), a non-ionic surfactant that does not interfere with ceramic dispersions [22], then foamed by vigorous mechanical mixing (2000 rpm). Foamed gels were kept at 75 °C for 24 h, in order to complete the curing, before being demoulded. Finally, hardened foamed gels were fired at 700 and 800 °C for 1 h with a heating rate of 1 °C/min or 10 °C/min. Selected samples were subjected to thermogravimetric analysis (TGA, STA409, Netzsch Gerätebau GmbH, Selb, Germany) and Fourier-transform infrared spectroscopy (FTIR, FTIR model 2000, Perkin Elmer Waltham, MA).

The geometric density of both hardened foamed gels and fired glass foams was evaluated by considering the mass to volume ratio. The apparent and the true density were measured by using a helium pycnometer (Micromeritics AccuPyc 1330, Norcross, GA), operating on bulk or on finely crushed samples, respectively. The three density values were used to compute the amounts of open and closed porosity.

The morphological and microstructural characterizations were performed by optical stereomicroscopy (AxioCam ERc 5 s Microscope Camera, Carl Zeiss Microscopy, Thornwood, New York, US) and scanning electron microscopy (FEI Quanta 200 ESEM, Eindhoven, The Netherlands). The pore size distribution of the foams was evaluated by means of image analysis using the Image J software [23]. The mineralogical analysis was conducted by X-Ray Diffraction analysis (XRD) on powdered samples (Bruker D8 Advance, Karlsruhe, Germany – CuKα radiation, 0.15418 nm, 40 kV–40 mA, 2θ = 10–70°, step size 0.05°, 2 s counting time). The phase Identification was performed by means of the Match!® program package (Crystal Impact GbR, Bonn, Germany), supported by data from PDF-2 database (ICDD-International Centre for Diffraction Data, Newtown Square, PA).

The obtained foams were subjected to compression tests by using an Instron 1121 UTS (Instron, Danvers, MA) machine, with a crosshead speed of 1 mm/min, employing samples of about 10 mm × 10 mm × 10 mm, cut from larger specimens (each data point corresponding to 10–12 samples).

3. Results and discussion

In order to study the gelation process the rheological behaviour of the mixtures was studied just after the alkali activation of the SL and then after every hour in oven at 75 °C. The flow curves obtained are plotted in Fig. 1a. The flow curves were analysed considering

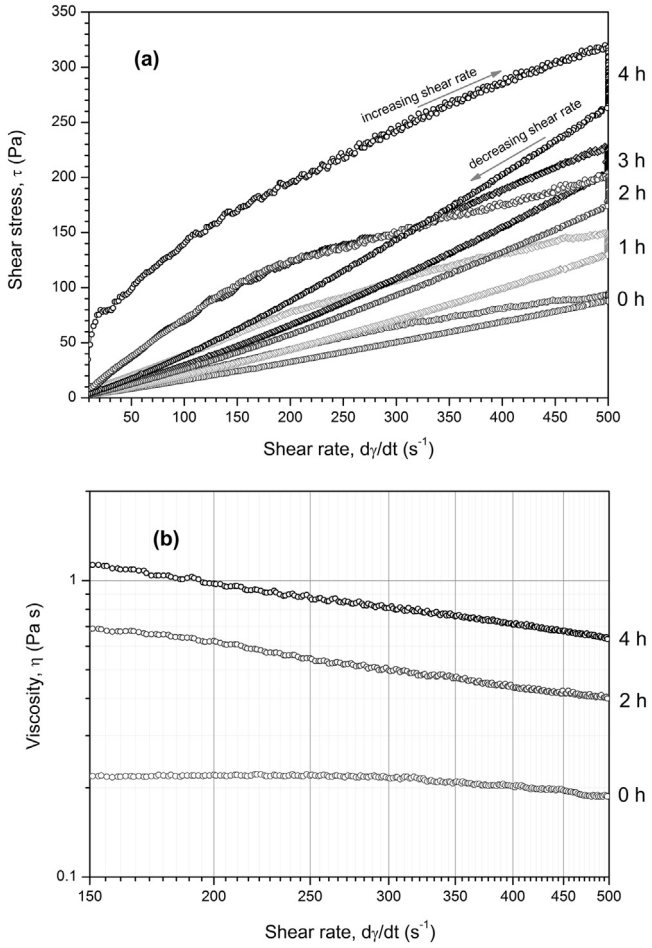

Fig. 1. a) Flow curves of suspensions of soda-lime glass (65 wt% solid content) after different gelation times; b) Viscosity plot for selected curing times.

different regression models; the best results were provided by the Herschel–Bulkley model, as follows:

$$\tau = \tau_0 + K \cdot \dot{\gamma}^n \quad (1)$$

where the shear stress (τ) is given by the sum of a yield stress (τ_0) and a factor depending on shear rate ($\dot{\gamma}$) ; K and n are constants referred to as consistency factor and flow behaviour index, respectively [24,25]. For a newtonian fluid the flow index is 1, whereas for a non-newtonian pseudoplastic fluid n is lower than 1.

The suspension prepared after only 3 h of mechanical stirring (before gelation) presented a narrow thixotropic cycle and low viscosity, both interpreted as indications of well-dispersed particles. As soon as the gelation process started, the thixotropic cycle became gradually larger and the viscosity increased; the interaction between components of suspensions caused viscous resistance, with a decrease of the flow index.

With a curing time of 1 h no foam could be achieved since the cellular structure determined by air incorporation collapsed rapidly, after interruption of mechanical stirring, by progressive coalescence of bubbles. On the contrary, with a curing time of at least 2 h, the transition from ongoing mechanical stirring (high shear rate) to interrupted mechanical stirring (shear rate equal to 0), determined an increase of viscosity that prevented the coalescence of bubbles. This shear-thinning behaviour can be understood from the viscosity plot in Fig. 1b. If we consider the viscosity, η, as the ratio between shear stress and shear rate, we can divide the exponential term of Eqn.1 by the shear rate:

$$\eta = \frac{\tau}{\dot{\gamma}} = K \cdot \dot{\gamma}^{n-1} \quad (2)$$

This can be rewritten as:

$$\mathrm{Log}\eta = \mathrm{Log}K + (n-1).\mathrm{Log}\ \dot{\gamma} \quad (3)$$

The linearity between viscosity and shear rate, in logarithmic scale, is confirmed by the same Fig. 1b. We can note the difference between the mixture just after the alkali activation (practically a newtonian fluid, with $1-n \approx 0$, i.e. $n \approx 1$, corresponding to an almost horizontal line) and after 2 h curing (n-$1 \approx -0.4$, i.e. $n \approx 0.6$).

After a prolonged curing the mixture actually corresponds, according to Fig. 1a, to a 'Bingham-pseudoplastic' fluid: since the interaction between surface gels formed at the surface of glass particles was particularly intense, the shear rate could increase only after the shear stress passed a threshold ('yield stress') of about 50 Pa. With the shear stress above this threshold, the decrease of viscosity with increasing shear rate is similar to the one for 2 h curing (Fig. 1b actually refers to an interval of shear rate values above the yield point).

The differences in the rheological behaviour with the duration of the curing step before foaming can be seen as a tuning parameter for the microstructure of 'green' foams, demoulded after 24 h of post-foaming curing, as shown by Fig. 2. The foams after 2 h exhibited a quite coarse microstructure, with many big interconnected pores surrounded by smaller ones, as an effect of coalescence between adjacent bubbles (Fig. 2a). The more pronounced pseudoplasticity with a longer curing step progressively reduced the coalescence (Fig. 2b,c); in particular, a curing step of 4 h was found to enhance the uniformity of foams (Fig. 2c).

Fig. 2f shows that the optimized curing time led to a quite narrow pore size distribution, centred at 500 μm, with a very limited fraction of pores having a diameter above 1 mm. In contrast, samples from a shorter curing (Fig. 2d,e), led to a wider pore size distribution, with significant fractions of pores exceeding 1 mm in diameter.

As expected, the materials after the post-foaming curing step were not chemically stable. When placed in distilled water, the foams led to a quite rapid increase of pH (up to ≈ 12), reasonably due to the release of alkali from the gels that previously caused the setting.

Fig. 3 represents the diffraction patterns of as-received soda-lime glass, hardened foams obtained after 2 and 4 h pre-foaming curing, and foams after firing at 700 and 800 °C. The patterns of the initial glass and those of the unfired foams do not allow for the detection of any crystalline phase. However, it could be noticed the shifting of the centre of the 'amorphous halo', from $2\theta = 24.40–26.30°$, for glass powders, to $2\theta = 28.40–30.40°$. This shift can be seen as a proof of the compositional changes determined by the alkaline activation of glass powder.

After the heat treatment (at 1 °C/min), at 700 °C, the structure remained amorphous, but the 'halo' moved back slightly to lower angles. In our opinion, this is consistent with the decomposition of the hydrated compounds and dissolution of oxides in new glass matrices, so that only the shift from alkali incorporation remained. In fact, the shift at higher angles (and lower reticular distance) is known to be correlated, in a glass, with the incorporation of network modifiers [18,26].

On the contrary, the heating at 800 °C determined a significant precipitation of sodium calcium silicates (mainly $3CaO{\cdot}Na_2O{\cdot}6SiO_2$ [PDF#77-0410], with traces of $4CaO{\cdot}2Na_2O{\cdot}6SiO_2$ [PDF#79-1086]). These silicates are well-known crystal phases formed upon devitrification of soda-lime glass, generally occurring at higher

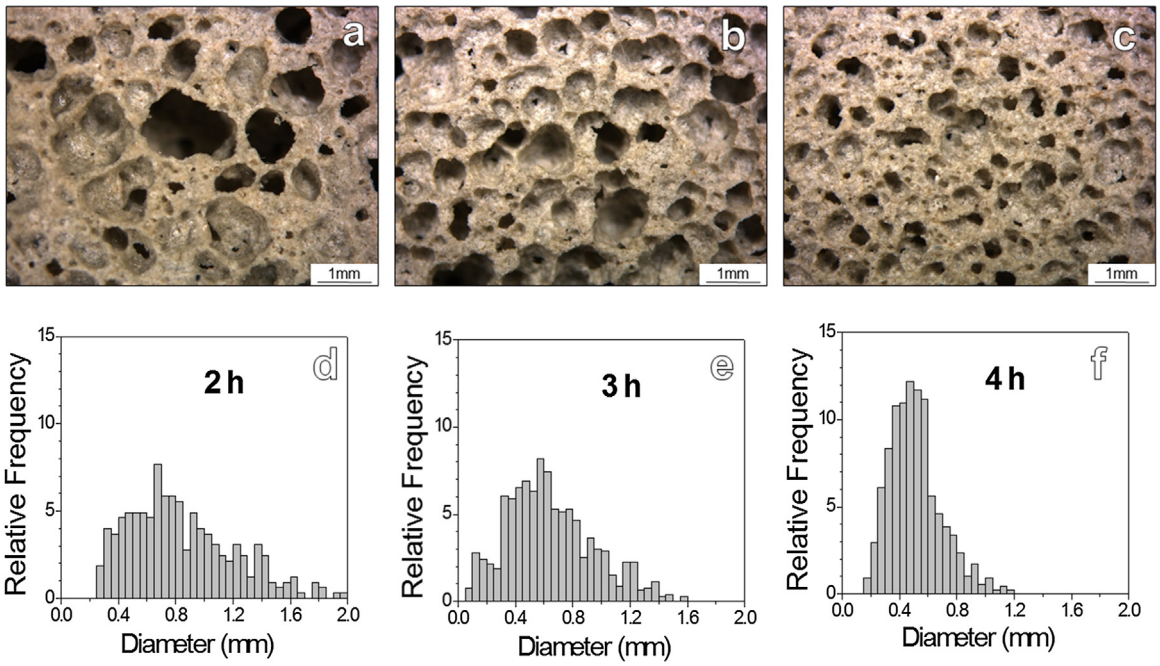

Fig. 2. Microstructural details and pore size distribution of hardened foamed gels.

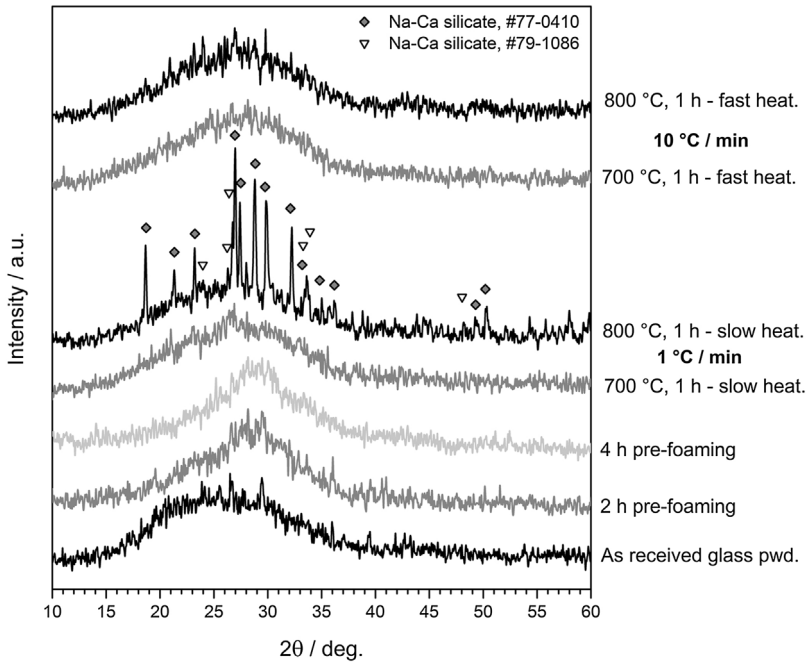

Fig. 3. X-ray diffraction patterns of glass foams at 'green state' and after firing.

temperatures [27]; the formation of an alkali-rich glass, from the decomposition of gels, evidently promoted the devitrification.

Some indications concerning the nature of the compounds developed upon curing and the related transformations, with the firing treatment, may come from infrared spectroscopy, as illustrated by Fig. 4. The wide peak in the 3000–3500 cm^{-1} interval, only in the FTIR spectrum of the 'green' glass foam (4 h prefoaming curing), in Fig. 4a, is consistent with the findings of Garcia Lodeiro et al. [28] concerning C-S-H gels in the presence of alkali. Also the peak at approximately 1450 cm^{-1} is consistent with what observed for C-S-H gels, namely it may be attributed to traces of carbonate compounds.

The slight weight losses above 500 °C, for gelified suspensions, as shown in Fig. 4b, are also consistent with the formation of hydrated compounds. In fact, these compounds are known to feature a distinctive thermal evolution, by removal of —OH groups, with water releases even up to high temperatures [29]. The more abundant weight losses at low temperature (below 500 °C), on the contrary, can be ascribed to both physically absorbed water and burn-out of surfactant. The additive cannot be the only reason for low temperature losses, as demonstrated by the plot for pure Triton X-100 in the same Fig. 4b (the plot for the surfactant is normalized according to the actual content of 4 wt%).

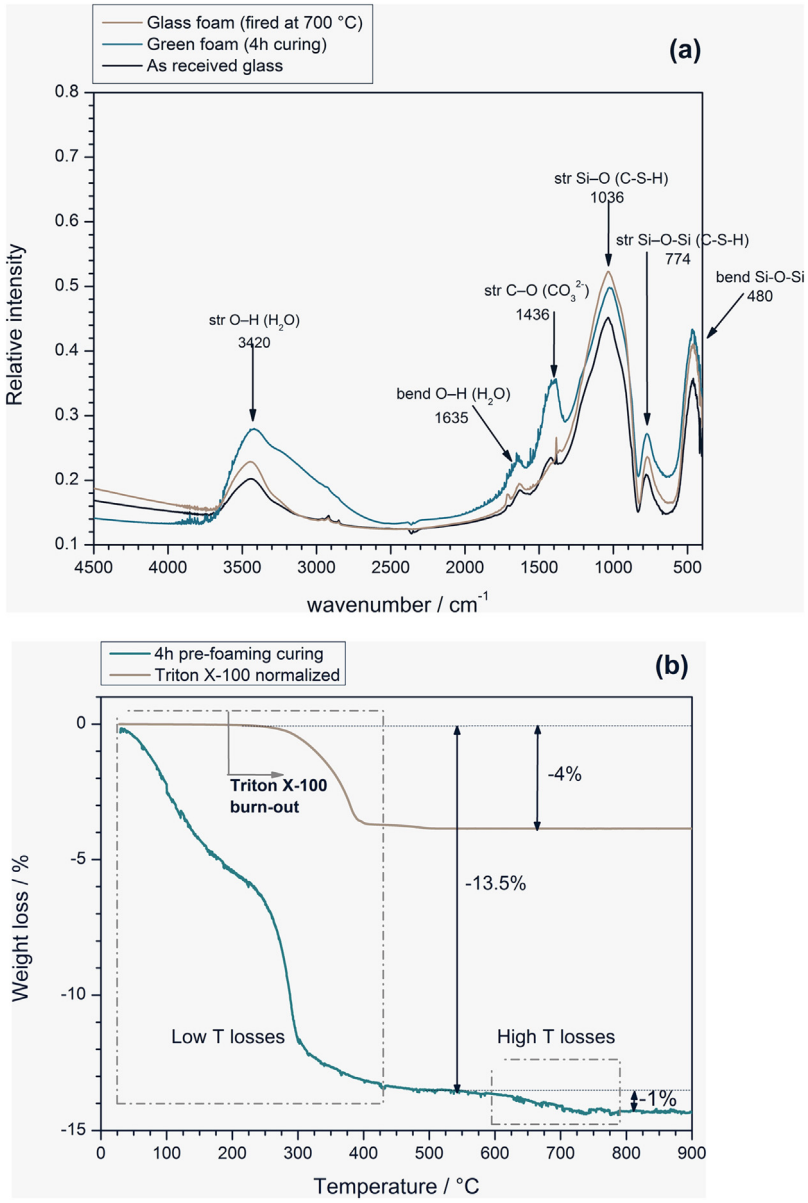

Fig. 4. a) FTIR spectra of selected materials; b) thermogravimetric plot of surfactant and gelified glass-based mixture.

The heat treatment at 700 and 800 °C – after a slow heating at 1 °C/min (aimed at the burn-out of the surfactant) – caused significant transformations in the cellular structures, especially for foams produced with short pre-foaming curing times. In these cases, the foams after firing are much more uniform: the foam produced at 700 °C with 2 h curing, as shown by Fig. 5a, features big pores surrounded by thick, micro-porous struts; the foam produced with 3 h curing, shown in Fig. 5b, becomes quite similar, in morphology, to the foam produced with 4 h curing. The foam with 4 h curing, in Fig. 5c, maintains a superior homogeneity, with only a limited fraction of pores with diameter above 400 μm. The pore size distributions of foams after firing, shown in Fig. 5d–f testify this evolution quantitatively. Analogous observation can be done on foams after firing at 800 °C, shown in Fig. 5g–l.

The transformations of the cellular structure is likely due to the above mentioned decomposition of hydrated compounds, which determined a 'secondary foaming'. 700 °C would be low, as firing temperature, for the foaming of soda-lime glass, but we must take into account the effect of alkali incorporation. Alkali-rich surface gels surrounding glass powders reasonably transformed into a low viscosity glass phase, acting as a 'glue' for undissolved material, promoting ionic inter-diffusion and finally favouring the secondary foaming by water release. The pronounced devitrification at 800 °C could be seen as an effect of ionic inter-diffusion from the original glass and the low viscosity glassy coating phase formed by decomposition of gels.

It is interesting to note that, from the reflected light in optical images, the foams after treatment at 700 °C feature closed 'membranes' between adjacent pores: the release of water vapour evidently led to closed pores, in analogy with the conventional sintering technology of glass foams (gas evolution upon sintering). This is confirmed by the density data in Table 1.

From the data in the same Table 1, the open porosity returned dominant at 800 °C. This is not a contradiction with the conditions at 700 °C; in fact, the foaming of glass is not a 'static' process, simply involving cell nucleation, in the pyroplastic mass of softened glass, and growth. Bubbles may collapse and be replaced by new ones, formed later. Fig. 6, as an example, shows a comparison between

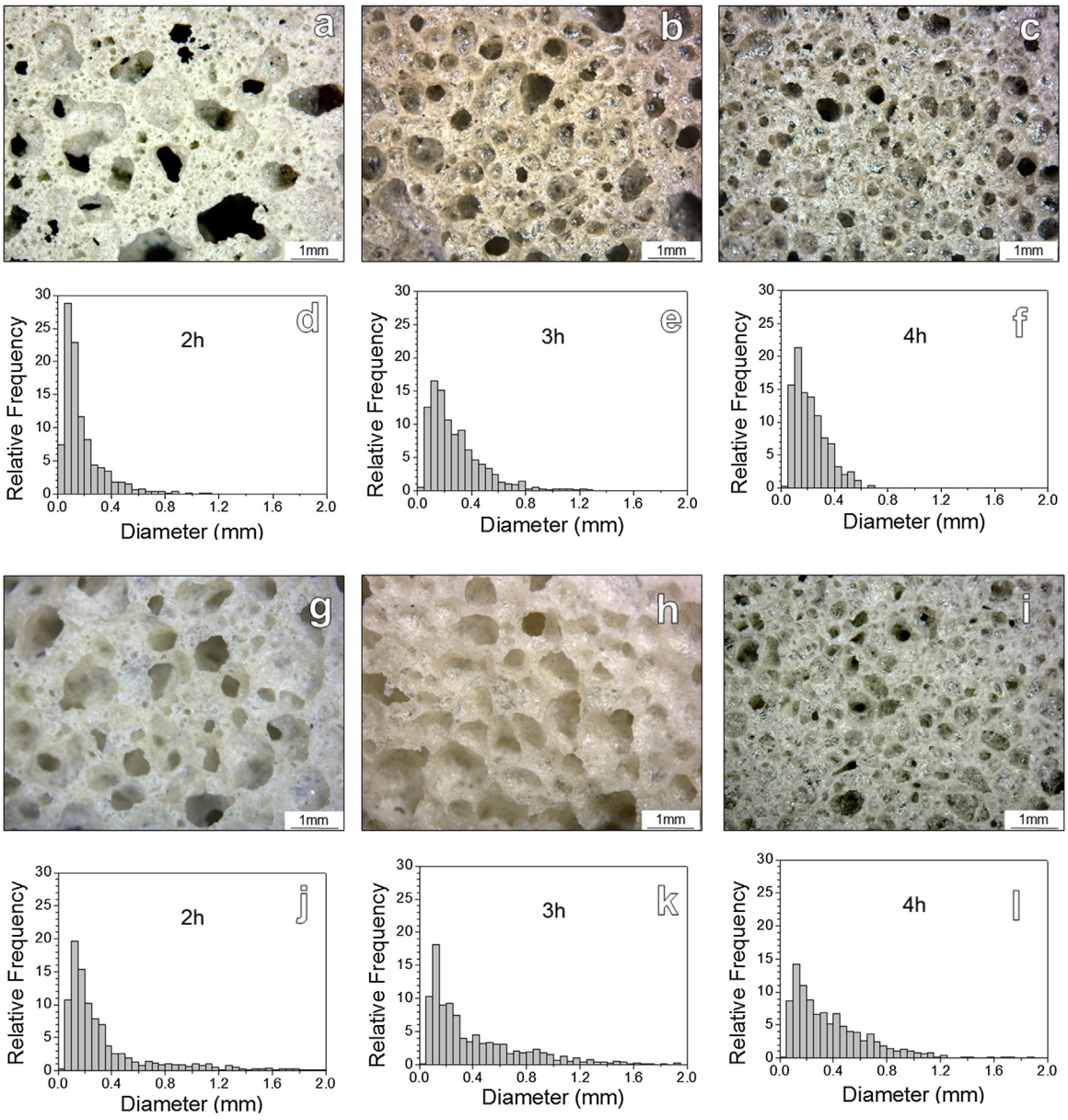

Fig. 5. Microstructural details and pore size distribution of glass foams after firing at 700 °C (a–f) and 800 °C (g–l) [slow heating rate].

Table 1
Density data of selected foams before and after heat treatment.

	2 pregel			3pregel			4 pregel			4 pregel	
	green 1 °C/min	700 °C	800 °C	green	700 °C	800 °C	green	700 °C	800 °C	700 °C 10 °C/min	800 °C
Density (g/cm^3)											
Bulk [ρb]	0.74 ± 0.02	0.26 ± 0,03	0.21 ± 0.03	0.67 ± 0.01	0.27 ± 0.02	0.27 ± 0.01	0.57 ± 0.01	0.30 ± 0.01	0.28 ± 0.01	0.34 ± 0.03	0.17 ± 0.01
Apparent [ρa]	2.08 ± 0.03	0.55 ± 0.03	2.73 ± 0.05	2.14 ± 0.06	0.45 ± 0.02	2.42 ± 0.02	2.29 ± 0.04	0.43 ± 0.06	2.41 ± 0.05	0.48 ± 0.08	2.41 ± 0.06
True [ρt]	2.11 ± 0.02	2.50 ± 0.01	2.89 ± 0.01	2.22 ± 0.02	2.44 ± 0.05	2.73 ± 0.01	2.31 ± 0.02	2.50 ± 0.02	2.66 ± 0.03	2.50 ± 0.03	2.66 ± 0.04
Porosity											
Total porosity [TP]	64.99 ± 0.04	89.62 ± 0.05	92.75 ± 0.02	69.95 ± 0.05	88.95 ± 0.09	89.95 ± 0.05	75.52 ± 0.05	88.11 ± 0.07	89.34 ± 0.03	86.34 ± 0.09	93.35 ± 0.11
Open porosity [OP]	64.44 ± 0.05	52.6 ± 0.1	92.3 ± 0.1	68.76 ± 0.06	38.6 ± 0.1	88.68 ± 0.07	75.28 ± 0.04	31.05 ± 0.09	88.25 ± 0.06	29.03 ± 0.11	84.10 ± 0.15
Closed porosity [CP]	0.55 ± 0.03	36.99 ± 0.04	0.45 ± 0.02	1.19 ± 0.02	50.15 ± 0.07	1.28 ± 0.03	0.24 ± 0.06	57.05 ± 0.02	1.09 ± 0.03	57.30 ± 0.156	9.33 ± 0.10

struts after firing at 700 (Fig. 6a) and 800 °C (Fig. 6b). The strut at 700 °C contains several small pores, with small openings; the low open porosity could be ascribed to the fact that the openings did not determine continuous paths. The small pores at the struts likely merged with increasing firing temperature, forming bigger pores like the one shown in Fig. 6b; the crystallization blocked the re-shaping of pores, by local increase of viscosity (softened glass turned into a suspension with rigid inclusions, represented by crystals), impeding the formation of continuous walls (the pore is evidently open).

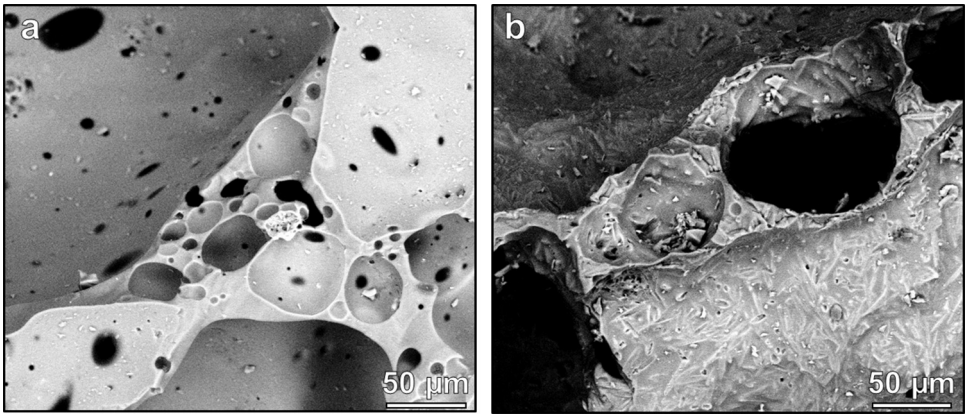

Fig. 6. High magnification details of glass foams after firing at: a) 700 °C; b) 800 °C [2 h pre-curing, slow heating rate].

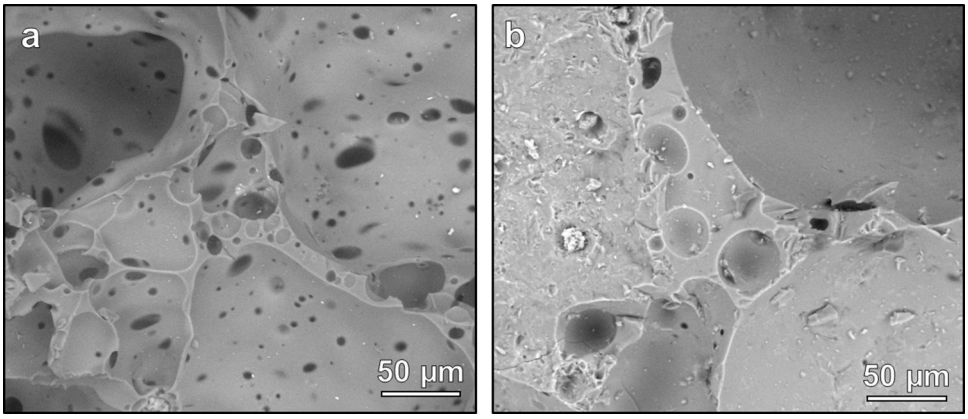

Fig. 7. High magnification details of glass foams after firing at: a) 700 °C; b) 800 °C [4 h pre-curing, high heating rate].

With a higher heating rate (10 °C/min), the foams treated remained practically amorphous even at 800 °C (see the X-ray diffraction pattern in Fig. 3); however, the effect of remodelling by viscous flow was so intensive that cells had a significant coarsening (see Fig. 7). The high amount of open porosity could be an artefact, i.e. it could be due not to a system of interconnecting pores, but to gas occupying very large bubbles at the surface of tested samples.

The different microstructures had an impact on the mechanical properties. The compressive strength of a glass foam is typically a function of the relative density, according to the well-known Gibson and Ashby model:

$$\sigma_f \approx \sigma_{bend} \cdot f(\Phi, \rho_{rel}) = \sigma_{bend} \cdot [C \cdot (\Phi \cdot \rho_{rel})^{3/2} + (1 - \Phi) \cdot \rho_{rel}] \quad (4)$$

where f is a 'structural function', depending on the relative density (ρ_{rel}, the ratio between the measured density of the foams and the true density, i.e. the density of the solid phase) and its distribution (open or closed porosity). The quantity $(1 - \Phi)$ expresses the fraction of solid positioned at the cell faces; if the foam is open-celled, the pores are fully interconnected with material only on the cell edges, so that $\Phi = 1$ $(1 - \Phi = 0)$. For closed cell foam, Φ is lower, with the solid phase constituting mostly cell walls and thus enhancing the linear term. C is a dimensionless calibration constant (~0.2). The reference soda lime glass bending strength σ_{fs} is 70 MPa, a typical value for container glass [8].

From Fig. 8 it is evident that the more homogeneous samples, with 4 h pre-foaming curing, fired at 700 °C in both heating modes, can be seen as the best, since they exhibited a crushing strength of more than 3 MPa with an overall porosity well above 85%. Although microporous, the membranes between adjacent cell walls were mechanically collaborating, so that the data are fitted by Φ well

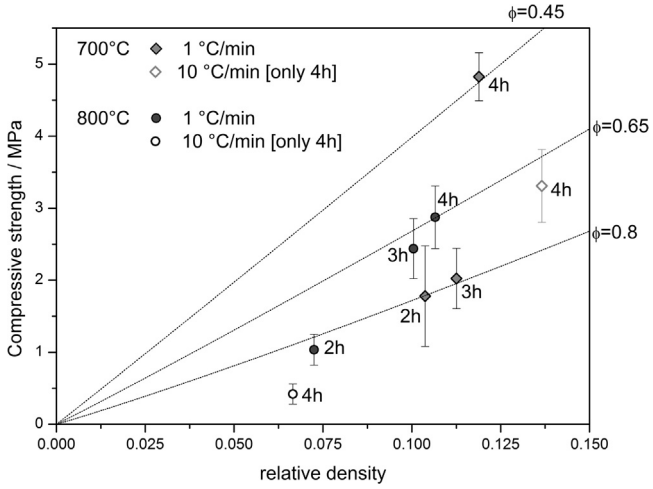

Fig. 8. Strength/relative density correlation for selected glass foams.

below 1. Firing at 800 °C had contrasting effects: while foams fired at slow heating rates were still particularly strong, despite the high porosity (nearly 90%), owing to the remarkable crystallization, the foams fired at high heating rate were quite weak (Φ above 0.8), owing to the very coarse cellular structure.

Firing treatments at low heating rate are probably difficult to be applied at an industrial scale. In any case, the foams corresponding to the firing at 700 °C, with a more industrially viable heating rate of 10 °C/min, compare favorably with commercial products. In particular, the specific strength (σ_f/ρ) of these foams approaches

10 MPa cm^3/g, a level exhibited only by the best variant of commercial Foamglas® [7]. The weak foams fired at 800 °C actually remain quite comparable to other commercial foams (foams of similar density possess a compressive strength of 400–800 kPa [30,31]).

Unlike commercial foams, the newly developed ones do not need any machining after firing. While Foamglas® [7] is cut into regular panels starting from big blocks, foams from our 'inorganic gel casting' process may be shaped directly operating on the geometry of moulds; in addition, 'green' foams can be machined easily before firing.

Further studies will be probably needed, in order to evaluate the durability of the products and explore the many combinations of process parameters (e.g. processing times and temperatures, heating rates, concentration and type of surfactant, solid content and glass composition) that evidently arise. Concerning durability, a preliminary test on the foam fired at 700° (10 °C/min), immersed in distilled water, demonstrated no increase of pH (the pH, from neutral value of 7, actually decreased to 6.5 after 10 days of immersion), as a result of the incorporation of alkali in the glass structure. The chemical stability should be actually assessed depending on all processing parameters; besides firing parameters, the adoption of ionic surfactants (instead on the non-ionic surfactant used in this investigation) may imply a modification of the overall alkali content.

4. Conclusions

We may conclude that:

- A new generation of glass foams may be obtained by alkali activation of suspensions of glass particles and gel-casting.
- The hardening of glass-based slurries is caused by the formation of C-S-H gels ('inorganic gel-casting').
- The cellular structure can be tuned depending on both rheology of gelified suspensions and firing treatments.
- Surfactants affect the morphology of 'green' foams, but do not determine 'secondary foaming'; the secondary foaming depends on decomposition of hydrated compounds (and possibly other compounds developed upon hardening, e.g. minor traces of carbonate compounds).
- A huge number of combinations of processing parameters is still to be explored (chemistry of glasses, surfactants, activating solution, curing times, conditions for heating treatments etc.).

Acknowledgement

The authors gratefully acknowledge the support of the European Community's Horizon 2020 Programme through a Marie Skłodowska-Curie Innovative Training Network ("CoACH-ETN", g.a. no. 642557).

References

[1] Press release European Container Glass industry welcomes long awaited circular economy package. Using waste as a secondary raw material in a closed loop is key Brussels, 02 December 2015.
[2] R. Beerkens, G. Kers, E. van Santen, Recycling of post-Consumer glass: energy savings, CO_2 emission reduction, effects on glass quality and glass melting, in: Anonymoused (Ed.), 71 st Conference on Glass Problems, John Wiley & Sons, Inc., 2011, pp. 167–194.
[3] G. Bonifazi, S. Serranti, Imaging spectroscopy based strategies for ceramic glass contaminants removal in glass recycling, Waste Manage. 26 (2006) 627–639.
[4] A. Farcomeni, S. Serranti, G. Bonifazi, Non-parametric analysis of infrared spectra for recognition of glass and glass ceramic fragments in recycling plants, Waste Manage. 28 (2008) 557–564.
[5] G. Meylan, H. Ami, A. Spoerri, Transitions of municipal solid waste management Part II: Hybrid life cycle assessment of Swiss glass-packaging disposal, Resour. Conserv. Recycling 86 (2014) 16–27.
[6] G. Scarinci, G. Brusatin, E. Bernardo, Glass foams, in: M. Scheffler, P. Colombo (Eds.), Cellular Ceramics: Structure, Manufacturing, Properties and Applications, WILEY-VCH Verlag GmbH & Co. KGaA, Weinheim, 2005, pp. 158–176.
[7] http://uk.foamglas.com/.../frontend/handler/document.php?id=131&type=42. (Accessed January 2017).
[8] A.S. Llaudis, M.J.O. Tari, F.J.G. Ten, E. Bernardo, P. Colombo, Foaming of flat glass cullet using Si_3N_4 and MnO_2 powders, Ceram. Int. 35 (2009) 1953–1959.
[9] J.L. Provis, Geopolymers and other alkali activated materials: why, how, and what? Mater. Struct. 47 (2014) 11–25.
[10] I. Lancellotti, E. Kamseu, M. Michelazzi, L. Barbieri, A. Corradi, C. Leonelli, Chemical stability of geopolymers containing municipal solid waste incinerator fly ash, Waste Manage. 30 (2010) 673–679.
[11] K. Garbev, L. Black, G. Beuchle, P. Stemmermann, Inorganic polymers in cement based materials, Wasser-und Geotechnologie 1 (2002) 19–30.
[12] I. Garcia-Lodeiro, A. Fernández-Jimenez, P. Pena, A. Palomo, Alkaline activation of synthetic aluminosilicate glass, Ceram. Int. 40 (2014) 5547–5558.
[13] I. Garcia-Lodeiro, E. Aparicio-Rebollo, A. Fernández-Jimenez, A. Palomo, Effect of calcium on the alkaline activation of aluminosilicate glass, Ceram. Int. 42 (2016) 7697–7707.
[14] C. Ruiz-Santaquiteria, A. Fernández-Jiménez, A. Palomo, Alternative prime materials for developing new cements: alkaline activation of alkali aluminosilicate glasses, Ceram. Int. 42 (2016) 9333–9340.
[15] F. Puertas, M. Torres-Carrasco, Use of glass waste as an activator in the preparation of alkali-activated slag. Mechanical strength and paste characterisation, Cem. Concr. Res. 57 (2014) 95–104.
[16] R. Redden, N. Neithalath, Microstructure, strength, and moisture stability of alkali activated glass powder-based binders, Cem. Concr. Compos. 45 (2014) 46–56.
[17] M. Torres-Carrasco, F. Puertas, Waste glass in the geopolymer preparation Mechanical and microstructural characterisation, J. Clean. Prod. 90 (2015) 397–408.
[18] M. Cyr, R. Idir, T. Poinot, Properties of inorganic polymer (geopolymer) mortars made of glass cullet, J. Mater. Sci. 47 (2012) 2782–2797.
[19] M. Strozi Cilla, P. Colombo, M.R. Morelli, Geopolymer foams by gelcasting, Ceram. Int. 40 (2014) 5723–5730.
[20] Z.Y. Wu, R.G. Hill, S. Yue, D. Nightingale, P.D. Lee, J.R. Jones, Melt-derived bioactive glass scaffolds produced by a gel-cast foaming technique, Acta Biomater. 7 (2011) 1807–1816.
[21] M. Marangoni, I. Ponsot, R. Kuusik, E. Bernardo, Strong and chemically inert sinter crystallised glass ceramics based on Estonian oil shale ash, Adv. Appl. Ceram. 113 (2) (2014) 120–128.
[22] X. Wang, J. Ruan, Q. Chen, Effects of surfactants on the microstructure of porous ceramic scaffolds fabricated by foaming for bone tissue engineering, Mater. Res. Bull. 44 (2009) 1275–1279.
[23] https://imagej.nih.gov/ij/. (Accessed July 2016).
[24] L. Bergstrom, Rheology of concentrated suspensions, Surfactant Sci. Ser. 51 (1993) 193–244.
[25] L.E. Vieira, J.B. Rodrigues Neto, A.N. Klein, R. Moreno, D. Hotza, Rheological and structural characterization of Ni–SiO_2 nanocomposites produced by aqueous colloidal processing, J. Am. Ceram. Soc. 94 (2011) 4179–4183.
[26] R. Hemmings, E. Berry, On the glass in coal fly ashes: recent advances, in: MRS Proceedings, Cambridge Univ Press, 1987, pp. 3.
[27] P. Hrma, D. Smith, J. Matyáš, J.D. Yeager, J.V. Jones, E.N. Boulos, Effect of float glass composition on liquidus temperature and devitrification behaviour, Phys. Chem. Glasses-Eur. J. Glass Sci. Technol. Part B 47 (2006) 64–76.
[28] I. García Lodeiro, A. Fernández-Jimenez, A. Palomo, D.E. Macphee, Effect on fresh C-S-H gels of the simultaneous addition of alkali and aluminium, Cem. Concr. Res. 40 (2010) 27–32.
[29] Q. Zhang, G. Ye, Dehydration kinetics of Portland cement paste at high temperature, J. Therm. Anal. Calorim. 110 (2012) 153–158.
[30] http://www.misapor.ch//. (Accessed January 2017).
[31] http://www.glapor.de/. (Accessed January 2017).